Biometals (2016) 29:467–485
DOI 10.1007/s10534-016-9929-1

Pyoverdine and histicorrugatin-mediated iron acquisition in *Pseudomonas thivervalensis*

Sandra Matthijs · Nathalie Brandt · Marc Ongena · Wafa Achouak · Jean-Marie Meyer · Herbert Budzikiewicz

Received: 20 November 2015 / Accepted: 19 March 2016 / Published online: 23 March 2016

Abstract The genome of *Pseudomonas thivervalensis* LMG 21626^T has been sequenced and a genomic, genetic and structural analysis of the siderophore mediated iron acquisition was undertaken. *Pseudomonas thivervalensis* produces two structurally new siderophores, pyoverdine PYO_{thi} which is typical for *P. thivervalensis* strains and a closely related strain, and the lipopeptidic siderophore histicorrugatin which is also detected in *P. lini*. Histicorrugatin consists out of an eight amino acid long peptide which is linked to octanoic acid. It is structurally related to the siderophores corrugatin and ornicorrugatin. Analysis of the proteome for TonB-dependent receptors identified 25 candidates. Comparison of the TonB-dependent receptors of *P. thivervalensis* with the 17 receptors of its phylogenetic neighbor, *P. brassicacearum* subsp. *brassicacearum* NFM 421, showed that NFM 421 shares the same set of receptors with LMG 21626^T, including the histicorrugatin receptor. An exception was found for their cognate pyoverdine receptor which can be explained by the observation that both strains produce structurally different pyoverdines. Mass analysis showed that NFM 421 did not produce histicorrugatin, but the analogue ornicorrugatin. Growth stimulation assays with a variety of structurally distinct pyoverdines produced by other *Pseudomonas* species demonstrated that LMG 21626^T and NFM 421 are able to utilize

Electronic supplementary material The online version of this article (doi:10.1007/s10534-016-9929-1) contains supplementary material, which is available to authorized users.

S. Matthijs (✉) · N. Brandt
Institut de Recherches Microbiologiques-Wiame, Campus du CERIA, 1 avenue Emile Gryson, bât 4B, 1070 Brussels, Belgium
e-mail: slmatthi@ulb.ac.be

M. Ongena
Walloon Center for Industrial Biology, University of Liège/Gembloux Agro-Bio Tech, Gembloux, Belgium

W. Achouak
Laboratory of Microbial Ecology of the Rhizosphere and Extreme Environments (LEMIRE), Aix-Marseille Université, CEA, CNRS, UMR 7265 Biosciences and biotechnology Institute of Aix-Marseille (BIAM), ECCOREV FR 3098, CEA/Cadarache, St-Paul-Lez-Durance, France

J.-M. Meyer
Département Génétique Moléculaire, Génomique, Microbiologie, UMR, 7156, CNRS/Université Louis-Pasteur, 28 rue Goethe, 67000 Strasbourg, France

H. Budzikiewicz
Institut für Organische Chemie, Universität zu Köln, Greinstrasse 4, 50939 Cologne, Germany

almost the same set of pyoverdines. Strain NFM 421 is able utilize two additional pyoverdines, pyoverdine of *P. fluorescens* Pf0–1 and *P. citronellolis* LMG 18378^T, these pyoverdines are probably taken up by the FpvA receptor of NFM 421.

Keywords Histicorrugatin · Pyoverdine · TonB-dependent receptor · *Pseudomonas thivervalensis* · *Pseudomonas brassicacearum* · Genome

Introduction

Most microorganisms produce siderophores when they are faced with iron-limiting conditions. Fluorescent pseudomonads produce a yellow–green, fluorescent siderophore, called pyoverdine (Meyer and Abdallah 1978). The structures of pyoverdines produced by different strains of fluorescent pseudomonads have been characterized. They are made of three distinct structural parts: a small peptide chain of L- and D-amino acids (6–14 amino acids depending on the producing strain), linked to a yellow–green chromophore group and a small dicarboxylic acid or its monoamide connected amidically to the NH_2-group of the chromophore (Budzikiewicz 1997). Pyoverdines contain catechol, hydroxamic and/or β-hydroxy amino acid groups that are participating in Fe^{3+} binding, the chromophore contains one catechol group, and the peptide chain the hydroxamic and β-hydroxy amino acid groups.

Besides pyoverdine, other secondary siderophores, which have a relatively lower affinity for iron, have been identified in fluorescent pseudomonads (Cornelis and Matthijs 2002). These include pyochelin, pseudomonine and thioquinolobactin (Cox and Graham, 1979; Mercado-Blanco et al. 2001; Matthijs et al. 2004, 2007). In addition the non-fluorescent *P. corrugata* has been reported to produce the lipopeptidic siderophore corrugatin (Risse et al. 1998). Corrugatin consists out of an eight amino acid long peptide which is linked to octanoic acid, an eight-carbon saturated fatty acid (Risse et al. 1998). Ten years after the description of the structure of corrugatin an analogue of corrugatin has been identified and annotated as ornicorrugatin (Matthijs et al. 2008) since the second diaminobutyric acid monomer of corrugatin is replaced by ornithine. Ornicorrugatin was isolated from *Pseudomonas* sp. AF76 (Matthijs et al. 2008), a *Pseudomonas* strain belonging to the *P. fluorescens* group. This siderophore is also produced by *P. fluorescens* SBW25 (Cheng et al. 2013) and a putative ornicorrugatin gene cluster has been proposed to be present in *Pseudomonas* sp. CH-C52 and *P. fluorescens* Q8r1-96 (Van Der Voort et al. 2015).

Siderophores trap traces of Fe^{3+} under the form of very stable complexes. After these siderophore-Fe complexes have been formed, they are internalized into the cells by specific TonB-dependent membrane receptors. *Pseudomonas* strains are able to use a variety of different siderophores produced by other micro-organisms, including fungi and bacteria (Poole et al. 1990; Jurkevitch et al. 1992; Raaijmakers et al. 1995; Hartney et al. 2011). They can also use heterologous pyoverdines, i.e. structurally different pyoverdines produced by other fluorescent pseudomonads. Growth stimulation assays with heterologous pyoverdines demonstrated that *P. entomophila* L48^T, *P. protegens* Pf-5 and *P. fluorescens* ATCC 17400 are able to utilize a large variety of structurally distinct pyoverdines (Matthijs et al. 2009; Hartney et al. 2011; Ye et al. 2014a). In contrast, *P. putida* KT2440 is able to utilize only its own pyoverdine and the pyoverdine produced by *P. syringae* (Matthijs et al. 2009).

In this study we show that under iron limiting conditions *P. thivervalensis* LMG 21626^T produces histicorrugatin, a siderophore structurally related to corrugatin and ornicorrugatin. In addition the structure elucidation of a new pyoverdine, PYO_{thi}, is described. Analysis of the draft genome revealed the putative siderophore biosynthetic and uptake gene clusters which were confirmed through the construction and characterization of mutants. The ability to take up exogenous siderophores was also investigated. Screening of the genome sequence of LMG 21626^T for genes coding for TonB-dependent receptors identified 25 candidates. Growth stimulation assays with heterologous pyoverdines demonstrated that *P. thivervalensis* is able to utilize a variety of structurally distinct pyoverdines produced by other *Pseudomonas* species. The TonB-receptors and the pyoverdine uptake profiles were compared to the ones of the phylogenetically closely related strain *P. brassicacearum* subsp. *brassicacearum* NFM 421. These were surprisingly similar, reflecting their genetic similarities.

Materials and methods

Bacterial strains and growth conditions

The *Pseudomonas* strains (Table 1) were routinely grown at 28 °C on an in house medium, medium 853 (Matthijs et al. 2013) or casamino acids (CAA). When required CAA was supplemented with $FeCl_3$ to a final concentration of 50 μM. *Escherichia coli* was grown in 853 at 37 °C. The antibiotics chloramphenicol (Cm), kanamycin (Km) and tetracycline (Tc) were used at a concentration of 25, 50 and 20 μg ml^{-1}, respectively.

Sequencing and annotation of the *P. thivervalensis* LMG 21626^T genome

Illumina paired-end sequencing was performed by Beckman Coulter Genomics (UK). The 100 bp reads were *de novo* assembled using Velvet (Zerbino and Birney 2008) using a minimum contig length cut-off of 1 kb and various k-mer lengths. This resulted in 59 contigs with in total 58 gaps between scaffolded contigs. The gaps were re-amplified by PCR using Fermentas DreamTaqGreen PCR enzyme. To assemble some of the 59 contigs together, outgoing primers were designed and a PCR was carried out (Fermentas DreamTaqGreen). The amplicons were sequenced using Sanger sequencing technique at Beckman Coulter Genomics (UK). During this work the genome sequence of *P. thivervalensis* DSM 13194^T was deposited (accession umber NZ_LHVE00000000.1), some of the contigs were assembled together (order of the contigs) based on that sequence. The draft genome sequence of *P. thivervalensis* LMG 21626^T has been deposited at DDBJ/EMBL/GenBank under accession number LRSO00000000. Annotation of open reading frames (ORF) was performed with the NCBI Prokaryotic Automatic Annotation Pipeline (PGAAP).

In silico analyses of siderophore gene clusters and TonB-receptors of *P. thivervalensis* LMG 21626^T

The gene clusters for pyoverdine and histicorrugatin biosynthesis and transport, and the TonB-receptors of *P. thivervalensis* were found by BLAST homology and search by keywords. The program NRPSpredictor2 (http://www.nrps.informatik.uni-tuebingen.de) which uses the methods of Stachelhaus et al. (1999) and Rausch et al. (2005) was used to predict the peptide backbone of the pyoverdine and histicorrugatin.

Construction of 21626^{T}ΔpvdL, 21626^{T}ΔhcsA, 21626^{T}ΔhcsEF, 21626^{T}ΔpvdLΔhcsEF in-frame deletion mutants of *P. thivervalensis* LMG 21626^T

A pyoverdine-negative deletion mutant was constructed in *P. thivervalensis* LMG 21626^T by deleting a 10.9 internal portion of the 13.0 kb *pvdL* gene. Therefore, 1 kb fragments from each of the 5′- and the 3′-end of *pvdL* were PCR amplified from LMG 21626^T using the primer pairs pvdL-AF and pvdL-AR, and pvdL-BF and pvdL-BR (Table 2), respectively. The resulting 5′- and the 3′-ends were cut with the restriction enzymes *Hin*dIII and *Xba*I and with *Xba*I and *Eco*RI, respectively, and cloned by triple ligation into *Eco*RI and *Hin*dIII-digested pUK21 (Km^R) (pUK-pvdL21626^T). The 2055-bp *Eco*RI–*Hin*dIII insert was verified by sequencing and recloned into the suicide plasmid pME3087 (Tc^R) (pME-pvdL21626^T). The resulting plasmid was then integrated into the chromosome of strain LMG 21626^T by triparental mating using *E. coli* HB101/pME497 as the mobilizing strain, with selection for Tc- and Cm resistant recombinants. Excision of the vector by a second crossing-over occurred after enrichment for Tc-sensitive cells (Schnider-Keel et al. 2000). The obtained mutant was verified by PCR and checked for loss of fluorescence in the iron-limiting media CAA.

Using the same approach in-frame deletion mutants were constructed for the histicorrugatin biosynthetic genes *hcsEF* (21626^{T}ΔhcsEF) and the histicorrugatin receptor *hcsA* (21626^{T}ΔhcsA), with the difference that the upstream and downstream flanking regions of the gene(s) to be deleted were amplified and not the 5′ and 3′ end (Table 2). For the double mutant 21626^T-ΔpvdLΔhcsEF the *pvdL* gene was deleted in the 21626^{T}ΔhcsEF mutant.

Chrome azurol S assay

Siderophore production was detected by the chrome-azurol S (CAS) assay (Schwyn and Neilands 1987). On CAS-agar, siderophores remove iron from CAS, resulting in a blue to yellow–orange color change in zones surrounding the colonies. Therefore, 10 μl of an overnight culture adjusted to $OD_{600} = 0.5$ was plated

Table 1 The strains used in this study

Strain/plasmid	Relevant genotype/characteristics	References
P. thivervalensis		
LMG 21626^T	Wild type, isolated from rhizoplane of *Brassica napus* (Nancy, France), produces PYO_{thi} and histicorrugatin	Achouak et al. (2000)
21626^{T}ΔpvdL	Pyoverdine-negative deletion mutant of *P. thivervalensis* LMG 21626^T, produces histicorrugatin	This study
21626^{T}ΔhcsA	Histicorrugatin TonB-receptor (*hcsA*)-negative deletion mutant of *P. thivervalensis* LMG 21626^T, produces PYO_{thi} and histicorrugatin	This study
21626^{T}ΔhcsEF	Histicorrugatin-negative *hcsEF* deletion mutant of *P. thivervalensis* LMG 21626^T, produces PYO_{thi}	This study
21626^{T}ΔpvdLΔhcsEF	Pyoverdine/histicorrugatin-negative deletion mutant of *P. thivervalensis* LMG 21626^T	This study
P. thivervalensis DR5	Endophyte isolated from field-grown *Solanum nigrum*, produces PYO_{thi} and histicorrugatin	Long et al. (2008)
P. thivervalensis MLG19	Isolated from *Arabidopsis thaliana* (Yvelines Thiverval Grignon, France), produces PYO_{thi} and histicorrugatin	Achouak et al. (2000)
P. thivervalensis MLG39	Isolated from *Arabidopsis thaliana* (Yvelines Thiverval Grignon, France), produces PYO_{thi} and histicorrugatin	Achouak et al. (2000)
P. thivervalensis MLG45	Isolated from *Arabidopsis thaliana* (Yvelines Thiverval Grignon, France), produces PYO_{thi} and histicorrugatin	Achouak et al. (2000)
P. thivervalensis R1-4	Rhizosphere oilseed rape, produces PYO_{thi}	Gasser et al. (2009)
P. brassicacearum subsp. *brassicacearum* NFM 421	Isolated from *Arabidopsis thaliana* plants growing in soils from Méréville, France. Produces pyoverdine ($PYO_{ATCC39167}$) and ornicorrugatin	Achouak et al. (2000)
NFM421-4D1	Pyoverdine-negative Tn5 mutant of *P. brassicacearum* subsp. *brassicacearum* NFM 421, Tc^R, produces ornicorrugatin	This study
P. brassicacearum BGCR2-9(1)	Endophyte from field-grown *Solanum nigrum*, produces PYO_{thi} and ornicorrugatin	Long et al. (2008)
P. lini LMG 21625^T	Isolated from rhizosphere soil of Dijon (*Linum usitatissinum*), produces pyoverdine and histicorrugatin	Delorme et al. (2002)
Pseudomonas sp. GM50	Isolated from root of *Populus deltoides*	Brown et al. (2012)
pUK21	Cloning vector; *lacZ*α; Km^R	Vieira and Messing (1991)
pME3087	Suicide vector, ColE1 replicon, RK2-Mob, Tc^R	Voisard et al. (1994)
pME-pvdL	pME3087 containing the 5′ and 3′ end of *pvdL*, Tc^R	This study
pME-hcsA	pME3087 containing the 5′ and 3′ flanking regions of *hcsA*, Tc^R	This study
pME-hcsEF	pME3087 containing the 5′ and 3′ flanking regions of *hcsEF*, Tc^R	This study

on CAA–CAS agar, kept at 28 °C for 48 h and the size of the halo was measured.

Large scale purification of PYO_{thi} and histicorrugatin of *P. thivervalensis* LMG 21626^T

Pyoverdine and histicorrugatin were purified from 72 h old culture supernatant of respectively *P. thivervalensis* LMG 21626^T and the pyoverdine-negative mutant 21626^{T}ΔpvdL, grown at 28 °C in three 4 l Erlenmeyer flasks containing 1 l of iron-poor CAA medium at 200 rpm. Bacterial cells were removed by centrifugation at 10,000*g* during 15 min. After filtration the supernatant was passed on a C-18 column that was activated with methanol and washed with distilled water. Elution was done with acetonitrile/H_2O (70/30 %). Most of the acetonitrile was

Table 2 The primers, and their sequence, used for the amplification of fragment A and B for the construction of plasmid pUK-pvdL21626^T, pUK-hcsA21626^T and pUK-hcsEF21626^T are given

Primer name	Primer sequence
Plasmid pUK-pvdL21626^T	
Amplification of fragment A (AF and AR) and B (BF and BR):	
pvdL-AF	5′-GTG*AAGCTT*GACCGACGCGTTCGAACT-3′
pvdL-AR	5′-GTG*TCTAGA*ACCCGCAACGAAGGAATG-3′
pvdL-BF	5′-GTG*TCTAGA*AGCGATGCCACCGGAACT-3′
pvdL-BR	5′-GTG*GAATTC*CCTCCAACTCCGCCATCA-3′
Verification primers of deletion	
pvdL-delF	5′-CACGATCTGGAACAGGTAACT-3′
pvdL-delR	5′-TGGCCTTGGTCCAGGTAGT-3′
Plasmid pUK-hcsA21626^T	
Amplification of fragment A (AF and AR) and B (BF and BR):	
hcsA-AF	5′-GTG*AAGCTT*CACTGGCCTTGATGCAATG-3′
hcsA-AR	5′-GTG*TCTAGA*GCCAACGCAATTGTGTTCT-3′
hcsA-BF	5′-GTG*TCTAGA*CCTGCGCTACGACATGTAA-3′
hcsA-BR	5′-GTG*GAATTC*CGACAGGTTGCCGCTGAT-3′
Verification deletion	
hcsA-delF	5′-GTCCTGGCAGTAGCGTTCA-3′
hcsA-delR	5′-CGTTCAATGTGACCGCTTGA-3′
Plasmid pUK-hcsEF21626^T	
Amplification of fragment A (AF and AR) and B (BF and BR):	
hcsEF-AF	5′-GTG*AAGCTT*GCAAGGCATGACCTTGTTCA-3′
hcsEF-AR	5′-GTG*CTGCAG*CACGATAGACATAATGGCATC-3′
hcsEF-BF	5′-GTG*CTGCAG*GACGAGGCCAACCTGTGAA-3′
hcsEF-BR	5′-GTG*TCTAGA*CTGCTCGTCGAGGTGAATC-3′
Verification deletion	
hcsEF-delF	5′-GCAGCATGACCTGCTGTTGA-3′
hcsEF-delR	5′-GTTGATGAACAGGCCGATCA-3′

Restriction enzymes sites are italics. In addition the primers, and their sequence, used to confirm the obtained deletions ΔpvdL, ΔhcsA and ΔhcsEF (verification deletion) are given

evaporated with a rotavapor and the samples were lyophilized.

Preparative-scale purification was done on a Prep 150 LC system (Waters). A SunFire Prep C18 column (C-18, 19 × 250 mm, 5 µm particle size) was used with a flow rate of 20 ml/min and a gradient going from H_2O/CH_3CN 9:1 containing 0.1 % CF_3COOH to H_2O/CH_3CN 2:8 containing 0.1 % CF_3COOH in 30 min. From the extract CH_3CN was evaporated *in vacuo* and the sample was lyophilized.

LC/MS analyses were performed on a Kontron 325 system, coupled to the mass spectrometer and equipped with a UV detector (model 322), an automatic injector (model 465) and LC-6A type pumps. The column used was a Vydac 218TP54 RP column (C_{18}, 5 µm, d = 0.46 cm, l = 25 cm) and a flow rate of 1 ml/min was maintained. Mass spectral data (MS) were recorded on a VG Quattro II spectrometer (ESP ionization, cone voltage 70 V, capillary voltage 3.5 kV, source temperature 80 °C). Data collection was done with Masslynx software.

Amplification and sequencing of housekeeping genes of non type *P. thivervalensis* strains

The almost complete 16S rRNA gene sequence (position 29–1522 in *E. coli*) of non type *P. thivervalensis* strains and *P. brassicacearum* BGCR2-9(1) was amplified with primers pA and pH (Edwards et al. 1989). Part of the housekeeping genes *gyrB* and *rpoD* was amplified using primers UP1E/APrU (Yamamoto et al. 2000) and PsEG30F/PsEG790R (Mulet et al. 2009), respectively. The PCR was carried out in a final volume of 25 µl containing PCR buffer (Qiagen) with

0.625 U *Taq* DNA polymerase (Qiagen), 5 µl Q-solution (Qiagen), the deoxynucleotide mixture at 100 µM (Fermentas), each of the primers at 0.5 µM (Sigma) and 1–2 µl template DNA. Template DNA for PCR reaction was purified using the DNeasy Blood and Tissue kit of Qiagen. The PCR program used was an initial denaturation of 2 min at 94 °C, followed by 40 cycles of denaturation at 94 °C for 30 s, annealing at 55 °C for 30 s and extension at 72 °C for 90 s for 16S rRNA, and 50 s for *gyrB* and *rpoD*, followed by an incubation for 10 min at 72 °C. The obtained PCR fragments were purified and sequenced at Beckman Coulter Genomics (UK) using amplification and internal primers (for 16S rRNA).

Phylogenetic analysis

Phylogenetic analysis based on concatenated almost complete 16S rRNA gene sequences and partial *gyrB* and *rpoD* genes was performed using CLUSTALX and MEGA v5.0 (Tamura et al. 2011). The neighbor-joining method was used with the Jukes-Cantor model and topological robustness was evaluated by bootstrap analysis based on 1.000 replicates. The 16S rRNA, *gyrB* and *rpoD* gene sequences of the type strains were taken from GenBank.

Using neighbor-joining analysis an unrooted tree was generated from the amino acid sequences of the TonB-dependent receptors of *P. thivervalensis* LMG 21626^{T} and *P. brassicacearum* subsp. *brassicacearum* NFM 421, with bootstrap support from 500 resampled datasets. The TonB-dependent receptors were identified by means of search by keywords including TonB, receptor, ligand gated channel and siderophore, and blast analysis.

Histicorrugatin gene cluster of *Pseudomonas* sp. GM50

The putative histicorrugatin gene cluster of *Pseudomonas* sp. GM50 was located on two different contigs, AKJK00000000 (5′ part) and AKJK01000000 (3′ part). By means of PCR with primers GM50-F1 (5′-CCGCTGTTCCAGGTGATGT-3′) and GM50-R3 (5′-GCTTCGTCGAGGATGTACA-3′) using DreamTaqGreen (Fermentas) an amplicon with the sequence linking both contigs together was obtained. The amplicon was sequenced (accession number KT748760 gives the sequence of the fragment after removal of the overlapping sequence of the contigs) and the fragments AKJK00000000, KT748760 and AKJK01000000 were concatenated.

Plasposon mutagenesis of *P. brassicacearum* NFM 421

The plasposon mutagenesis method (Dennis and Zylstra 1998) was used to generate transposon insertions in the chromosome of *P. brassicacearum* NFM 421. Mid-log phase cultures of *E. coli* SM10 (λpir), the host of the plasposon pTnmod-OTc, was mixed with strain NFM 421 in a 1:1 ratio. *P. brassicacearum* was kept at 37 °C for 1 h just before mixing of both strains in order to inactive its restriction system. After overnight incubation on 853 at 28 °C, transposon insertions in strain *P. brassicacearum* were selected on CAA supplemented with 50 µg ml^{-1} Tc and 20 µg ml^{-1} Cm. A bank of 728 transconjugants was screened for mutants with a reduced or loss of the ability to produce pyoverdine as detected by reduction or loss of fluorescence. The mutants were characterized molecularly as described in (Matthijs et al. 2009).

Pyoverdine typing through IEF and mass analysis

The pyoverdine of the *Pseudomonas* strains (Table 3) was purified using the medium scale method as described in Matthijs et al. (2009). Pyoverdine-isoelectrofocusing was done with the Clean Gel IEF from GE Healthcare. For ampholines Pharmalyte pH 3 till 10 was used (GE Healthcare). The gel was prepared according the manufactor instructions with following minor modifications; the rehydradation of the gel was done with double volume and the ampholines concentration was increased by 25 %.

Utilization of exogenous pyoverdines by *P. thivervalensis* LMG 21626^{T} and *P. brassicacearum* subsp. *brassicacearum* NFM 421

Twenty ml CAA agar plates containing 400 µM of 2,2-dipyridyl were overlaid with 5 × 10^{7} cells of a fresh culture of the mutant 21626^{T}ΔpvdLΔhcsEF or NFM421-4D1, and filter-paper disks impregnated with 20 µl of 8 mM or 5 µl of 32 mM purified pyoverdine were placed on the agar. The plates were subsequently incubated at 28 °C and scored for the

Table 3 List of strains with the type of pyoverdine produced

Strain pyoverdine isolated from	Cross-feeding		Composition of pyoverdine peptide chain or siderotype	References or source
	21626^{T}ΔpvdLΔhcsEF	NFM421–4D1		
Six amino acids				
P. koreensis LMG 21318^{T}	–	–	Ala-Lys-Thr-Ser-AOHOrn-cOHOrn[a]	This study, Budzikiewicz et al. (1992)
P. lini W2Aug36	+	+	eLys-OHAsp-Ala-aThr-Ala-cOHOrn	Matthijs et al. (2009)
Seven amino acids				
P. aeruginosa 7NSK2	+	+	Ser-FOHOrn-Orn-Gly-aThr-Ser-cOHOrn[a] (Type II pyoverdine)	This study, Tappe et al. (1993)
P. libanensis LMG 21606^{T}	–	–	Ala-Orn-OHAsp-Ser-Orn-Ser-cOHOrn	Meyer et al. (2008)
P. putida BTP2	–	–	Ser-Val-OHAsp-Gly-Thr-Ser-cOHOrn	Ongena et al. (2001)
P. putida KT 2440	–	–	Asp-Orn-(OHAsp-Dab)-Gly-Ser-cOHOrn	Matthijs et al. (2009)
Pseudomonas sp. W15Feb38	+	+	Ser-AOHOrn-Ala-Gly-aThr-Ala-cOHOrn	Matthijs et al. (2009)
Eigth amino acids				
P. aeruginosa PAO1	–	–	Ser-Arg-Ser-FOHOrn-(Lys-FOHOrn-Thr–Thr) (Type I pyoverdine)	Briskot et al. (1989)
P. brassicacearum subsp. *brassicacearum* NFM 421	±	+	Ser-AOHOrn-Ala-Gly-(Ser-Ala-OHAsp-Thr)[a]	This study, Uría-Fernández et al. (2003)
P. chlororaphis D-TR133	+	+	Asp-FOHOrn-Lys-(Thr-Ala-Ala-FOHOrn-Ala)	Barelmann et al. (2003)
P. fluorescens Pf-5	+	+	Asp-FOHOrn-Lys-(Thr-Ala-Ala-FOHOrn-Lys)	Matthijs et al. (2009)
P. salomonii LMG 22120^{T}	+	+	Ser-Orn-FOHOrn-Ser-Ser-(Lys-FOHOrn-Ser)[a]	This study, Schlegel et al. (2001)
Nine amino acids				
P. fluorescens Pf0-1	–	+	Ala-AcOHOrn-Orn-Ser-Ser–Ser-Arg-OHAsp-Thr	Meyer et al. (2008)
P. lurida LMG 21995^{T}	+	+	Ser–Ser-FOHOrn-Ser-Ser-(Lys-FOHOrn-Lys-Ser)[a]	This study, Sultana et al. (2000)
P. costantinii LMG 22119^{T}	+	+	Ser-AOHOrn-Gly-aThr-Thr-Gln-Gly-Ser-cOHOrn[a]	This study, Fernández et al. (2001)
P. thivervalensis LMG 21626^{T}	+	+	Ala-AcOHOrn-Gly-Thr-Thr-Gln-Gly-Ser-cOHOrn	This study
Ten amino acids				
P. brenneri LMG 23068^{T}	–	–	Ser-Dab-Gly-Ser-OHAsp-Ala-Gly-Ala-Gly-cOHOrn	Matthijs et al. (2009)
P. entomophila L48^{T}	–	–	Ala-Asn-Dab-OHHis-Gly–Gly-Ala-Thr-Ser-cOHOrn	Matthijs et al. (2009)
P. fluorescens DSM 50106	–	–	Ser-Lys-Gly-FOHOrn-Ser–Ser-Gly-(Orn-FOHOrn-Ser)	Meyer et al. (2008)

Table 3 continued

Strain pyoverdine isolated from	Cross-feeding		Composition of pyoverdine peptide chain or siderotype	References or source
	21626^{T}ΔpvdLΔhcsEF	NFM421–4D1		
P. rhodesiae LMG 17764^T	+	+	Ser-Lys-FOHOrn-Ser-Ser-Gly-(Lys-FOHOrn-Ser–Ser)[a]	This study, Budzikiewicz (2004)
Twelve amino acids				
Pseudomonas sp. W15Oct28	–	–	Asp-Ala-AOHOrn-Thr-Gly-c(Thr-(O)-Hse-Hya-Ser-Orn-Hse-Ser-O)	Ye et al. (2013)
Unknown structures				
P. agarici LMG 2112^T	+	+		
P. asplenii LMG 21749^T	–	–		
P. cedrina LMG 23661^T	–	–		
P. chlororaphis W2Apr9	+	+		
P. citronellolis LMG 18378^T	–	+		
P. fluorescens LMG 14562	–	–		
P. mosselii LMG 21539^T	–	–		
Pseudomonas sp. W2Jun14	–	–		
Pseudomonas sp. W15Apr2	+	+		
Pseudomonas sp. W15Oct11	–	–		

Abbreviations used for uncommon amino acids, three letter code; *aThr* allo-Thr, *eLys* Lys linked by its e-NH_2, *AOHOrn* δN-acetyl-δN-hydroxy-ornithine, *FOHOrn* δN-formyl-δN-hydroxy-ornithine, *cOHOrn* cyclo-hydroxy-ornithine (3-amino-1-hydroxy-piperidone-2), *OHHis* threo-β-hydroxy-histidine, *OHAsp* threo-β-hydroxy-aspartic acid, *Dab* diamino-butanoic acid. Cyclic pyoverdines are indicated by parentheses

[a] The structure was deduced from the observation that the IEF profile and the mass of the pyoverdine was identical to the relevant reference strain

presence of detectable growth of the pyoverdine-negative mutant after 1 and 2 days.

Results

P. thivervalensis LMG 21626^T produces a new pyoverdine PYO_{thi}

From *P. thivervalensis* MLG45 a pyoverdine was isolated for which only the molecular mass, 1261 determined by mass spectrometry, has been reported (Meyer et al. 2008). A detailed study of the electrospray mass spectra (Budzikiewicz et al. 2007) allows to present the amino acid sequence of the pyoverdine: Ala-AcOHOrn-Gly-(a)Thr-(a)Thr-Gln-Gly-Ser-cOHOrn. Two isoforms were observed, for one of them with a succinamide (Suca) residue attached to the chromophore (Chr) the typical pattern for a Suca-Chr-Ala N-terminus was obtained by collision induced fragmentation of $[M + 2H]^{2+}$ as well as the sequence of b-ions (cleavage of the amide bonds) (Table 4). A differentiation between Thr and aThr is not possible, nor can the chirality of the amino acids be determined. A second isoform with malamide (Mala) attached to Chr yields $[M + H]^+$ with a mass of 1277 and a_1 shifted to 416 and losing 115 Da (Mala) instead of 99 Da (Suca). Through IEF and mass analysis the pyoverdine of LMG 21626^T was compared to the one of MLG45. Based on these results the pyoverdine structures of MLG45 and LMG 21626^T are identical.

To verify whether this pyoverdine is typical for *P. thivervalensis*, i.e. do they belong to the same siderotype (Meyer et al. 2002), 3 additional *P. thivervalensis* strains (Table 1), including 2 isolates (MLG19 and MLG39) from *Arabidopsis thaliana*

Table 4 Mass spectrometry data allowing a peptide chain structure proposal for PYO_{thi} of *P. thivervalensis* MLG45

	m/z value	$-NH_3$	$-H_2O$	$-CH_2CO$
A_1	400	383	382	
B_1	428		410	
B_2	600	583	582	558
B_3	657		639	
B_4	758		740	
B_5	859		841	
B_6	987		969	
B_7	1044		1026	
B_8	1131		1113	
M + H	1261		1243	
M + H $-NH_3$ $-H_2O$	1226			1184

Suca-Chr-Ala-AcOHOrn-Gly-(a)Thr-(a)Thr-Gln-Gly-Ser-cOHOrn

An isoform with Mala gives M + H 1277 and A_1 416

(Achouak et al. 2000) and a rhizosphere isolate (R1–4) from oilseed rape (Gasser et al. 2009), were analyzed by means of IEF and LC–MS. All these strains produced PYO_{thi} indicating that this pyoverdine is typical for *P. thivervalensis*. Sequencing of the almost complete 16S rRNA gene and partial *gyrB* and *rpoD* genes and subsequent phylogenetic analysis with the type strains of the *P. corrugata* subgroup (Mulet et al. 2010) confirmed for all strains, except strain R1–4, their identification as *P. thivervalensis* (Fig. 1).

Screening of an in house IEF data set of pyoverdine samples of a large collection of more than 450 strains revealed an additional strain, the endophyte *P. brassicacearum* BGCR2-9(1) from *Solanum nigrum* (Long et al. 2008), with the same IEF profile. LC–MS analysis confirmed that this strain also produces PYO_{thi}. *P. brassicacearum* BGCR2-9(1) clusters with strain *P. thivervalensis* R1-4. These results indicate that the ability to produce PYO_{thi} is specific for *P. thivervalensis* and a closely related species represented by *P. brassicacearum* BGCR2-9(1) and *P. thivervalensis* R1-4.

PYO_{thi} is structurally almost identical to the pyoverdine of *P. costantinii* (PYO_{cos}) (Fernández et al. 2001) (previously *P. tolaasii*-like isolate), the first amino acid of the peptide chain of the pyoverdine of *P. costantinii* is serine instead of alanine which gives mass differences of 16 for the B-series (Table 3). The structural similarity is reflected in the IEF profile of both pyoverdines (Fig. 2) which are highly similar. Pyoverdine-mediated ^{59}Fe-uptake showed that PYO_{cos} was taken up at similar levels (95 %, value

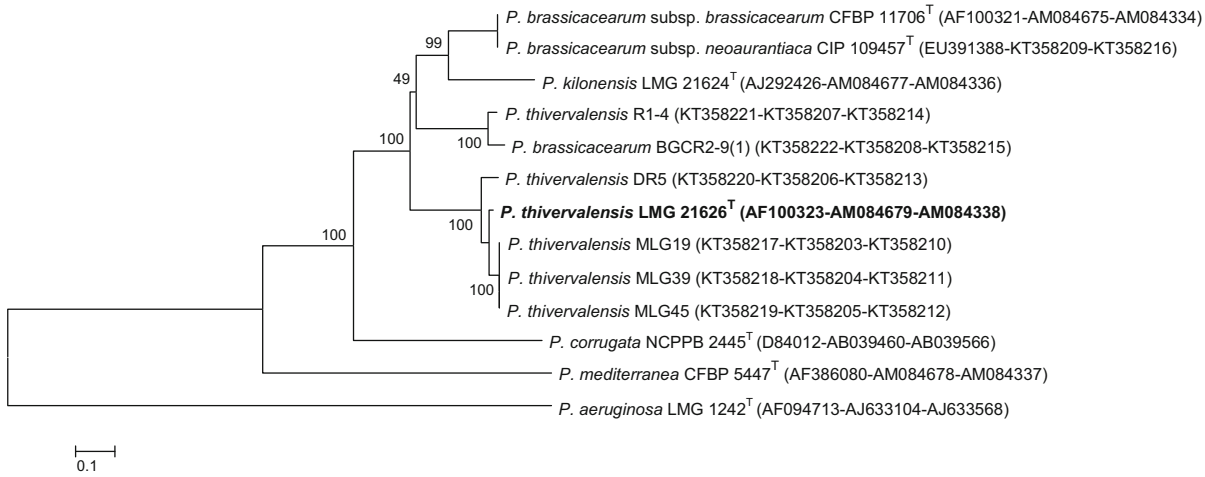

Fig. 1 Neighbor-joining tree based on concatenated almost complete 16S rRNA gene sequence and partial *gyrB* and *rpoD* gene sequences showing the position of *P. thivervalensis* strains LMG 21626^T (in *bold*), DR5, MLG19, MLG39 and MLG45. Distance matrices were calculated by the Jukes-Cantor method. *Pseudomonas aeruginosa* was used as outgroup. The *bar* indicates sequence divergence. *Bootstrap values* are indicated at *branch points*. Genbank accession numbers are given in *parentheses*

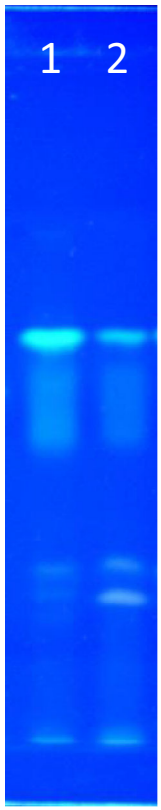

Fig. 2 Isolectrofocusing patterns of PYO_{thi} produced by *P. thivervalensis* LMG 21626^T (*1*) and pyoverdine produced by *P. costantinii* LMG 22119^T (*2*)

is expressed in percentage of incorporation compared to the homologous system) as PYO_{thi} by *P. thivervalensis* wild type strain.

A search of the draft genome sequence of *P. thivervalensis* LMG 21626^T revealed 25 genes involved in pyoverdine-mediated iron acquisition, transport and regulation which are distributed across three different loci of the genome. Based on in silico analysis of the 3 non-ribosomal peptide synthetases (NRPS) genes (APS14_17615-APS14_17630) (Fig. 3) a nine amino acid long peptide backbone was predicted. As observed for other *Pseudomonas* species, the chromophore NRPS gene *pvdL* (APS14_09630) is located at a separate locus (generally together with one enzyme involved of the modification of the peptide chain, and the sigma factor regulator PvdS) while the receptor gene *fpvA* (APS14_17610) is found at the same locus as the peptide chain biosynthesis genes (Moon et al. 2008). Deletion of *pvdL* in the mutant $21626^T\Delta$pvdL led to complete loss of pyoverdine production as confirmed by loss of fluorescence and loss of the pyoverdine pics in HPLC chromatogram. The pyoverdine-negative mutant was unable to grow on CAA supplemented with the strong iron chelator EDDHA.

P. thivervalensis LMG 21626^T produces the secondary siderophore histicorrugatin

The pyoverdine-negative mutant $21626^T\Delta$pvdL was still able to decolorize chrome azurol S, a large halo was observed after 48 h, suggesting the production of a second siderophore. The halo observed for the $21626^T\Delta$pvdL mutant is slightly reduced in comparison with the halo of the wild type.

The CAS-positive fraction of the pyoverdine-negative mutant $21626^T\Delta$pvdL was collected and purified by preparative HPLC. A siderophore, designated histicorrugatin, structurally related to corrugatin and ornicorrugatin was isolated. The mass of the $[M + H]^+$ ion was found to be 1034.5016 corresponding to a molecular formula of $C_{43}H_{68}N_{15}O_{15}$ (calc'd. 1034.5018). The mass difference relative to ornicorrugatin **2** ($[M + H]^+$ 1012) of 22 Da suggests that one of the β-hydroxyaspartic acid (OHAsp) units of the latter is replaced by β-hydroxyhistidine (OHHis). The lower mass region up to B3 (*m/z* 476) corresponds to that of ornicorrugatin (see discussion Matthijs et al. 2008) indicating identical partial structures of the two compounds up to the third N-terminal amino acid (Orn)—except for *m/z* 485 for **1** corresponding to *m/z* 463 in the spectrum of **2**. This ion represents Y''_5 after the loss of 74 Da (Supplementary Fig S1, loss of the side chain of OHAsp) from *m/z* 559, a mass increment of 22 Da in agreement with the exchange of one OHAsp by OHHis in the C-terminal part.

In the upper mass range besides $[M + H]^+$ (*m/z* 1034) elimination of the side chain of OHAsp (−74 Da, *m/z* 960), of OHHis (−96 Da, *m/z* 938) and of both (−170 Da, *m/z* 864)—see Supplementary Fig S1—is observed. All these ions are accompanied by the loss of one and two molecules of H_2O. Ions indicating the combined loss of H_2O and CO_2 (62 Da) from various precursors can be seen, viz. *m/z* 972 from 1034, 876 from 938, and the most pronounced one at *m/z* 802 arising from *m/z* 864. Of importance for the localization of the new OHHis unit (exchange of the first or third OHAsp starting from the C-terminus) is the ion *m/z* 711. It is shifted to *m/z* 697 for corrugatin and it is observed also at *m/z* 711 for ornicorrugatin.

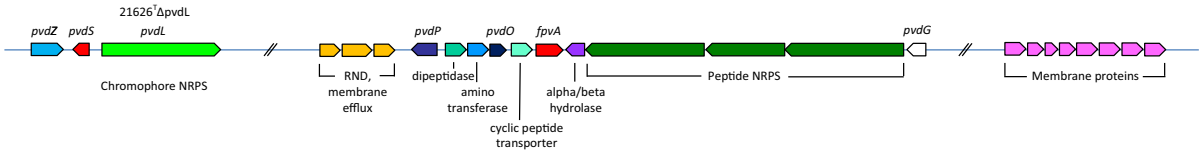

Fig. 3 The organization of the pyoverdine biosynthetic uptake and regulation gene cluster of *P. thivervalensis* LMG 21626^{T}. *Double vertical lines* represent intervening DNA

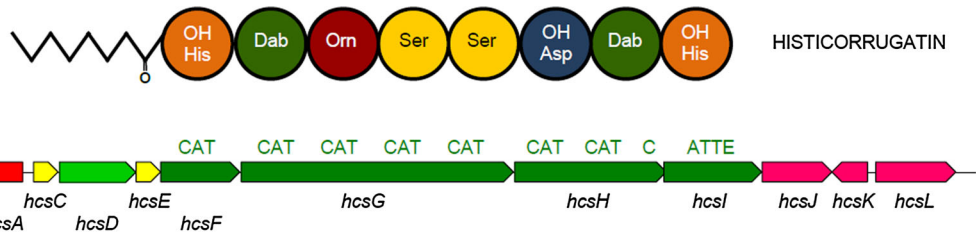

P. lini DSM 16768^{T}	91	81	91	87	95	84	90	90	84	94	81	91
P. lini ZBG1	91	81	91	87	95	84	90	90	84	94	81	91
Ps sp. GM50	94	80	91	95	95	82	91	91	84	95	--	40
Ps sp. 45MFCol3.1	94	85	93	86	96	83	89	90	85	96	--	39

Fig. 4 A schematic presentation of the structure of histicorrugatin and the histicorrugatin biosynthetic and uptake gene cluster of *P. thivervalensis* LMG 21626^{T}. The organization of the modules and domains in these four proteins is shown above the *arrows*. Below the gene cluster the similarities of the proteins of *P. thivervalensis* LMG 21626^{T} with translated gene products of *Pseudomonas* sp. GM50, *Pseudomonas* sp. 45MFCol3.1, *P. lini* LMG 21625^{T} and *P. lini* ZBG1 are shown. Similarities below 50 % are shown in red. The locus tags of the proteins are given in Supplementary Table S1

Therefore it contains the N-terminal parts of the molecules. It stems from the combined elimination (loss of 170 Da) of the side chains of OHAsp and OHHis from *m/z* 881 (this ion is more pronounced in the MS2-spectrum) which in turn is formed by the loss of the respective C-terminal amino acid with back-transfer of the OH group, in this case by the loss of 153 Da corresponding to OHHis (Fuchs and Budzikiewicz 2001). Kept in the solution obtained by elution of the sample from the column during purification histicorrugatin **1** decomposes after some time by elimination of the OHHis residue (96 Da), as observed in the mass spectra. The mass of the $[M + H]^{+}$ ion of the resulting species *m/z* 938.4692 corresponds to $C_{39}H_{64}N_{13}O_{14}$ (calc'd. 938.4695). Its mass spectrometric fragmentation corresponds to that discussed for the parent compound 1. Of importance is again *m/z* 711, here due to the loss of the OHAsp side chain only from *m/z* 785 which is formed by the elimination of 153 Da (see above).

A gene cluster for histicorrugatin biosynthesis and transport was found by searching the *P. thivervalensis* genome and BLAST homology. The gene cluster resides on a 42.1 kb fragment and includes 12 open reading frames (ORFs). The predicted function for each ORF was assigned by comparing the translated product with known proteins in public databases. Four non-ribosomal peptide synthetases (NRPS), designated HcsF, HcsG, HcsH, and HcsI (APS14_13800-APS14_13815) assemble the 8-residue histicorrugatin peptide backbone. The organization of the modules and domains in these four proteins is shown in Fig. 4. These eight modules adhere to the colinearity rule, specifying a colinear relationship between number and type of amino acids and the number and sequence of modules. In addition a thioesterase (TE) domain which catalyzes the release of NRPS product was found in the last protein *Hcs*I (Fig. 4).

Several non-proteinogenic amino acids were found in the peptide chain of histicorrugatin (Fig. 4). There are 2 L-Dab (2,4-diaminobutanoic acid) residues. These arise probably from HcsB (APS14_13840), a diaminobutyrate-2-oxoglutarate transaminase that catalyzes the reversible conversion of L-aspartate

4-semialdehyde + L-glutamate to L-2,4-diaminobutanoate + 2-oxoglutarate. In addition one ornithine residue was found in the peptide chain of histicorrugatin (Fig. 4). Genes directing the synthesis of this amino acid were not expected since ornithine is normally found in the bacterial cell as intermediate in arginine metabolism.

Several hydroxylated amino acids were found in the histicorrugatin backbone, at the first and last position an OHHis and at the sixth position an OHAsp (Fig. 4). These residues are most likely hydroxylated by the SyrP proteins HcsC (APS14_13830) and HcsE (APS14_13820) (Singh et al. 2008). Both SyrP proteins showed an identity of 43 % in a 294 residues overlap. At the N-terminal of the peptide chain of histicorrugatin a fatty acid is found (Fig. 4). HcsD (APS14_13825), similar to acyl-CoA synthetases (AMP-forming)/AMP-acid ligases, is predicted to act on the octanoid acid to synthesize an acyl-CoA derivate. The role of the gene cluster in histicorrugatin biosynthesis was confirmed through the construction of deletion mutants, deletion of 2 biosynthetic genes (*hcsEF*) in 21626^{T}ΔhcsEF and 21626^{T}ΔpvdLΔhcsEF resulted in complete loss of histicorrugatin production. Export of the siderophore from the cell is likely to involve HcsJ, HcsK and HcsL (APS14_13785-13795) predicted to function as components of ABC transporters (Fig. 4). Uptake of histicorrugatin probably occurs through the TonB-dependent receptor HcsA (APS14_13835) (Fig. 4). Deletion of the receptor in mutant 21626^{T}ΔhcsA resulted in a decreased production of histicorrugatin.

The double mutant 21626^{T}ΔpvdLΔhcsEF, unable to produce PYO_{thi} and histicorrugatin, showed a weak, diffuse CAS discoloration activity. If there is an alternative third iron uptake system it should have a rather low activity for iron.

By LC–MS analysis histicorrugatin was also detected in the *P. thivervalensis* strains DR5, MLG19, MLG39 and MLG45. Histicorrugatin was not detected in the closely related strain *P. brassicacearum* BGCR2-9(1), but the siderophore ornicorrugatin was found in its supernatant. By searching public databases a putative histicorrugatin biosynthetic and uptake gene cluster was found in *Pseudomonas lini* DSM 16768^{T}, *Pseudomonas lini* ZBG1, *Pseudomonas* sp. 45MFCol3.1 and *Pseudomonas* sp. GM50 (Fig. 4). Histicorrugatin was indeed detected in the culture supernatant of *P. lini* LMG 21625^{T}, but under the conditions used, histicorrugatin was not detected in the supernatant of strain GM50 (nor ornicorrugatin or corrugatin). The other 2 strains were not available and their siderophores produced could therefore not be verified.

In *Pseudomonas* sp. GM50 and 45MFCol3.1 the last two genes, a putative siderophore-iron reductase and a gene involved in transport of histicorrugatin, showed respectively no and a low similarity at the amino acid level to the translated genes *hcsK* and *hcsL* of *P. thivervalensis* LMG 21626^{T} (Fig. 4). But they were highly similar to each other (89 and 93 % identity at amino acid level, respectively) indicating that they have the same origin. Blast analysis showed only low levels of identity of these two genes of GM50 and 45MFCol3.1 with predominantly non *Pseudomonas* strains so it is not clear as where these genes are coming from. The presence of these 'atypical' genes might explain why no histicorrugatin production was observed in *Pseudomonas* sp. GM50. Nevertheless, these results show that histicorrugatin production is probably not rare and not limited to *P. thivervalensis* strains.

Utilization of exogenous pyoverdines by *P. thivervalensis* LMG 21626^{T} and *P. brassicacearum* subsp. *brassicacearum* NFM 421

Pseudomonas strains produce a limited number of siderophores but they are able to use many exogenous siderophores due to the presence of a multitude of receptors in their genome (Cornelis and Matthijs 2002). In addition to the cognate pyoverdine receptor FpvA and the histicorrugatin receptor an additional 23 TonB-dependent receptors were found in the LMG 21626^{T} proteome. For four of these receptors gene expression is probably controlled by ECF σ factors as indicated by the presence of extracytoplasmic sigma factors and transmembrane anti-σ factors adjacent to the receptor (Table 5). Based on Blast analysis a putative function could be attributed to five TonB dependent receptors, responsible for the uptake of ferrioxamine B, copper, heme, coprogen and rhodotorulic acid, and ferrichrome, respectively (Table 5).

Pseudomonas strains are also able to utilize pyoverdine from other fluorescent pseudomonads (Matthijs et al. 2009; Hartney et al. 2011; Ye et al. 2014a). To estimate the diversity of exogenous pyoverdines that may be utilized by *P. thivervalensis*

Table 5 TonB-dependent receptors found in the genome of *P. thivervalensis* LMG 21626^T, their putative role based on Blast analysis, presence of ECF sigma factor and the level of identity at amino acid level of their closest homologues in *P. brassicacearum* subsp. *brassicacearum* NFM 421

TonB-dependent receptors of LMG 21626^T	Residues	Function based on blast hit	ECF sigma	Level of identity (aa) to NFM 421
APS14_00155	834	Ferrioxamine B	Yes	97 % to PSEBR_a193
APS14_02400	708	Copper		98 % to PSEBR_a609
APS14_04030	782			94 % to PSEBR_a901
APS14_05530	864	Heme	Yes	95 % to PSEBR_a1204
APS14_06930	713			97 % to PSEBR_a3192
APS14_07200	210			89 % to PSEBR_a3239
APS14_07855	796		Yes	–
APS14_11280	715			–
APS14_11285	683			–
APS14_11650	807			95 % to PSEBR_a2949
APS14_11715	842			97 % to PSEBR_a2962
APS14_12340	667			–
APS14_12450	716			–
APS14_13415	803			–
APS14_13435	741			–
APS14_13835	687	Histicorrugatin		93 % to PSEBR_a2396
APS14_16155	722	FpvA		94 % to PSEBR_a3481
APS14_16900	825	Coprogen and rhodotorulic acid		95 % to PSEBR_a1921
APS14_17610	816	FpvA PYO_{thi}		38 % to PSEBR_a3917
APS14_18690	707			97 % to PSEBR_a4120
APS14_22195	701			95 % to PSEBR_a4729
APS14_23650	707			95 % to PSEBR_a2765
APS14_24450	626			95 % to PSEBR_a5030
APS14_25320	812	Ferrichrome	Yes	95 % to PSEBR_a5195
APS14_28280	730			–

LMG 21626^T, pyoverdines were purified from 31 different *Pseudomonas* strains and isolates (Table 3), which had been shown to each produce a unique siderotype profile (Meyer et al. 2008; Matthijs et al. 2009). The pyoverdines were supplied to the pyoverdine and histicorrugatin-deficient mutant 21626^T-ΔpvdLΔhcsEF that had been overlaid as a dilute suspension onto CAA medium containing 2,2-dipyridyl. Growth was clearly restored by provision of some of the purified pyoverdines, including the cognate pyoverdine PYO_{thi} (Table 3). Out of the other 30 pyoverdines tested, 13 were able to stimulate growth (Table 3), these included the pyoverdine of *P. agarici* LMG 2112^T, *P. brassicacearum* subsp. *brassicacearum* NFM 421, *P. chlororaphis* D-TR133, *P. chlororaphis* W2Apr9, *P. costantinii* LMG 22119^T, *P. lini* W2Aug36, *P. lurida* LMG 21995^T, *P. protegens* Pf-5, *P. rhodesiae* LMG 17764^T, *P. salomonii* LMG 22120^T, *Pseudomonas* sp. W15Apr2, *Pseudomonas* sp. W15Feb38 and type II pyoverdine of *P. aeruginosa* 7NSK2. These results show that *P. thivervalensis* can utilize a diverse set of pyoverdines as iron sources. The pyoverdine of *P. brassicacearum* subsp. *brassicacearum* NFM 421 was not able to fully restore growth in the conditions of the assay. In addition it has been observed that when the growth stimulation assay was repeated out in the presence of the strong iron chelator EDDHA (instead of 2,2-dipyridyl)

pyoverdine of NFM 421 cannot stimulate at all the growth of a pyoverdine-negative mutant of *P. thivervalensis*. Pyoverdine-mediated ^{59}Fe-uptake showed that the pyoverdine of NFM 421 was taken up at low levels (35 %, value is expressed in percentage of incorporation compared to the homologous system) by *P. thivervalensis* wild type strain.

Strain LMG 21626^{T} was not able to utilize type I pyoverdine produced by *P. aeruginosa* PAO1 and pyoverdines of strains of the *P. putida* group (Mulet et al. 2010) including *P. entomophila* L48^{T}, *P. putida* BTP2, *P. putida* KT2440, *P. putida* W15Oct28, *Pseudomonas* sp. W2Jun14 and *Pseudomonas* sp. W15Oct11 which all produce structurally different pyoverdines. In addition, LMG 21626^{T} was not able to utilize the pyoverdine of *P. cedrina*, *P. citronellolis*, *P. fluorescens* DSM 50106, *P. fluorescens* LMG 14562, and the type strain of *P. asplenii*, *P. brenneri*, *P. koreensis*, *P. libanensis* and *P. mosselii*.

P. thivervalensis is phylogenetically most closely related to *P. brassicacearum.* Therefore it was verified whether their phylogenetic relationship was reflected in the number and type of TonB-dependent receptors and whether there are large differences in their pyoverdine uptake profiles. IEF and LC–MS analysis showed that NFM 421 produces the same pyoverdine as *P. putida* ATCC 39167 (Uría-Fernández et al. 2003) (Table 3). Sequencing of 16S rRNA of ATCC 39167 revealed that the strain received as ATCC 39167 is not a *P. putida* strain, but belongs to the *P. fluorescens* group and is closely related to *P. brassicacearum*. Their 16S rRNAs (1278 bp) show a 99.7 % identity at nucleotide level.

Seventeen TonB-dependent receptors of NFM 421 were extracted from its genome and a phylogenetic tree was constructed with the 25 TonB-dependent receptors of LMG 21626^{T}. Interestingly, almost all the receptors of NFM 421 clustered with a homologue of *P. thivervalensis* (Fig. 5). The TonB-receptors showed very high identity levels at the amino acid level, values between 89 and 98 % were observed (Table 5). In fact only the cognate pyoverdine receptor of NFM 421, which showed only an identity of 38 % with the FpvA receptor of *P. thivervalensis* (Table 5), did not cluster with a homologue.

The histicorrugatin receptor of *P. thivervalensis* showed an identity of 93 % to PSEBR_a2396 of NFM 421. Histicorrugatin was not detected in the culture supernatant of NFM 421 but the analogue ornicorrugatin was found. Ornicorrugatin is produced by the gene cluster PSEBR_a2386-PSEBR_a2397 of NFM 421, Tn5 mutants in the nrps genes PSEBR_a2390 and PSEBR_a2391 lead to a complete loss of ornicorrugatin production (Matthijs S., *unpublished results*).

To compare the diversity of exogenous pyoverdines that may be utilized by both strains, growth stimulation assays were repeated as described above with the pyoverdine-negative mutant NFM421-4D1 of *P. brassicacearum* subsp. *brassicacearum* NFM 421. The pyoverdine utilization profiles of both strains are almost identical (Table 3). In contrast to the pyoverdine of NFM 421 which was not able to stimulate growth of *P. thivervalensis* very well, clear growth stimulation was observed of PYO_{thi} for *P. brassicacearum*. A difference in the utilization profiles of both strains was observed for the pyoverdine of *P. citronellolis* LMG 18378^{T} and *P. fluorescens* Pf0-1, these pyoverdines were only able to crossfeed *P. brassicacearum* (Table 3).

Discussion

P. thivervalensis sp. are typically plant-associated bacteria, they have been isolated as endophyte from *Solanum nigrum* (Long et al. 2008) and from *Arabidopsis thaliana* and *Brassica napus* roots (Achouak et al. 2000). This work shows that they produce the high affinity siderophore pyoverdine (PYO_{thi}) and the lipopeptidic siderophore histicorrugatin under iron limiting conditions to fulfill their need for iron. Iron is an essential element; it is a constituent of enzymes with critical roles in metabolism of hydrogen, oxygen or nitrogen, electron transfer, RNA synthesis and dissolution of reactive oxygen intermediates (Braun 1997). Acquisition of iron is complicated by the inherently low solubility of ferric iron, possible adsorption of Fe^{3+} on to colloids and precipitation of iron with other ions result in even lower iron concentrations in soil.

The production of iron-chelating siderophores by bacteria can be beneficial for the plant, because they can significantly increase the solubility of iron (Lemanceau et al. 2009). Nutritional competition for iron by the production of siderophores has been extensively studied as a mechanism of biological control. The plant growth-promoting effect of some

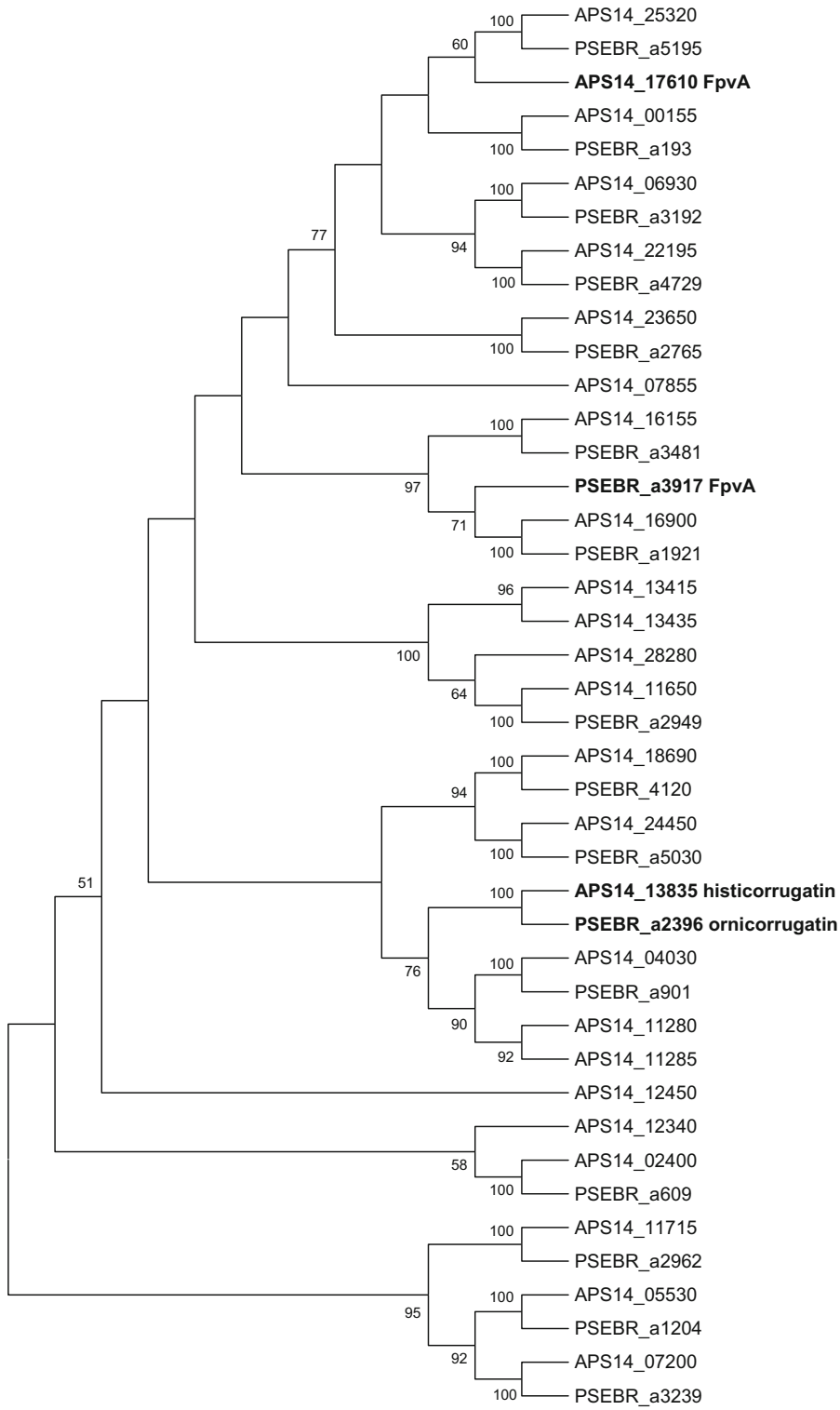

Fig. 5 Phylogenetic relationships among amino acid sequences of all the putative TonB-dependent receptors of *P. brassicacearum* NFM 421 and *P. thivervalensis* LMG 21626^{T}. The locus tag of each receptor is indicated on the tree. The tree was constructed using the NJ method. Numbers at nodes represent levels (%) of bootstrap support from 500 resampled datasets

fluorescent pseudomonads is thought to be in part due to siderophores, including pyoverdine, pyochelin and salicylic acid, that sequester iron in a form unavailable to deleterious micro-organisms in the rhizosphere, thereby preventing the pathogens' access to the already limited pool of soluble iron in the rhizosphere if the latter do not possess more efficient iron uptake systems (Kloepper et al. 1980; Höfte et al. 1991; Loper and Henkels 1997; Duijff et al. 1999). In addition, it has been observed that siderophores produced by fluorescent pseudomonads can trigger defense responses in the host (Maurhofer et al. 1994; Leeman et al. 1996; Bakker et al. 2007; De Vleesschauwer and Höfte, 2009).

Another trait, besides the ability to produce high affinity siderophore(s), which is important when microorganisms are competing for iron, is the ability to utilise iron complexes of a variety of different siderophores produced by other microorganisms, including fungi and bacteria (Poole et al. 1990; Jurkevitch et al. 1992; Raaijmakers et al. 1995). This "siderophore piracy" has two obvious advantages, the microorganism does not have to use metabolic energy for the synthesis of iron chelators, and by stealing the siderophore of other microorganisms it deprives these organisms of iron. It has been shown that *P. fluorescens* BBc6R8, in the presence of a coelichelin and desferrioxamines producing *Streptomyces* strain, did not produce pyoverdine but relied on utilisation of the siderophores produced by the *Streptomyces* strain (Galet et al. 2015). The capacity to utilise exogenous siderophores varies between *Pseudomonas* species and probably reflects the importance of iron competition in the natural habitat of the bacteria. Based on in silico analysis the receptors for the uptake of the siderophores ferrioxamine B, coprogen, rhodotorulic acid and ferrichrome could be attributed to *P. thivervalensis* LMG 21626^T.

Strain LMG 21626^T has in total 25 TonB-dependent receptors, eigth more than its phylogenetic neighbor *P. brassicacearum*. These numbers are on the lower side, especially for *P. brassicacearum* subsp. *brassicacearum* NFM 421 which has the lowest number of TonB-dependent receptors reported until now, but is in the same range as the phytopathogen *P. syringae* for which 19 (B728a) to 25 (DC3000) TonB-dependent receptors are found (Cornelis and Bodilis 2009). In contrast, the total number of genes coding for TonB-dependent receptors in the plant-associated *P. fluorescens* strains A506, SBW25 and *P. protegens* Pf-5 are respectively 34, 37 and 45 (Hartney et al. 2011). The highest number of TonB-dependent receptors has been found in *P. putida* W15Oct28 isolated from a small river (Matthijs et al. 2013), which has the amazing number of 56 genes coding for TonB-dependent receptors (Ye et al. 2014b). But what is intriguing when comparing the type of TonB dependent-receptors between *P. thivervalensis* and *P. brassicacearum* is that NFM 421 has the same pool of TonB-dependent receptors, except for the cognate FpvA receptor, as *P. thivervalensis*. *P. thivervalensis* has an additional 8 receptors, giving this strain probably a competitive advantage over *P. brassicacearum*. It would be interesting to study which type of compounds can be taken up by these additional TonB-dependent receptors.

Two pyoverdine receptors are found in *P. thivervalensis* LMG 21626^T and *P. brassicacearum* subsp. *brassicacearum* NFM 421, their cognate FpvA receptor and a putative second pyoverdine receptor (APS14_16155 and PSEBR_a3481, respectively). These receptors do not belong to the core genome, but to the accessory genome (Cornelis and Bodilis 2009). Pyoverdine growth stimulation assays showed that *P. thivervalensis* and *P. brassicacearum* are able to utilize respectively 13 and 15 structurally distinct pyoverdines produced by other *Pseudomonas* sp. out of 31 pyoverdines tested. This number is roughly comparable to the 17 pyoverdines *P. protegens* Pf-5 is able to utilize (Hartney et al. 2011). For *P. fluorescens* ATCC 17400 this was 20 out of 28 pyoverdines tested (Ye et al. 2014a) and for *P. entomophila* 16 out of 24 (Matthijs et al. 2009). Since sometimes different pyoverdines have been tested for these strains these data cannot be directly compared but they do indicate that many pyoverdines can be utilized by *P. thivervalensis*.

Despite the fact that the cognate FvpA receptors of *P. thivervalensis* and *P. brassicacearum* did not show large sequence similarities and did not cluster together in the phylogenetic tree of TonB-dependent receptors (Fig. 5), the pyoverdine utilisation profiles of *P. thivervalensis* and *P. brassicacearum* are almost identical. The observed differences in the uptake profiles of both strains, whereby NFM 421 can take up 2 additional pyoverdines, can probably be attributed to $FpvA_{NFM421}$. Through the construction of Fpv mutants the specificity and the level of redundancy of each

receptor can be further studied. The similarities in their uptake profile might reflect, besides their genetic similarities, their biological origin. Both strains were isolated in the same study, but from different plants and geographic environments; LMG 21626^{T} was isolated from *Brassica napus* and NFM 421 from *Arabidopsis thaliana* (Achouak et al. 2000). But in the latter study both *P. thivervalensis* and *P. brassicacearum* strains have been isolated from *B. napus* and *A. thaliana* (Achouak et al. 2000), which indicate that they are probably able to colonize the same host plant.

Acknowledgments The authors are indebted to Pelletier Dale, Baldwin Ian-Thomas and Gasser Ilona for generous gift of strains.

References

Achouak W, Sutra L, Heulin T, Meyer J-M, Fromin N, Degraeve S, Christen R, Gardan L (2000) *Pseudomonas brassicacearum* sp. nov. and *Pseudomonas thivervalensis* sp. nov., two root-associated bacteria isolated from *Brassica napus* and *Arabidopsis thaliana*. Int J Syst Evol Microbiol 50:9–18

Barelmann I, Fernandez DU, Budzikiewicz H, Meyer JM (2003) The pyoverdine from *Pseudomonas chlororaphis* D-TR133 showing mutual acceptance with the pyoverdine of *Pseudomonas fluorescens* CHA0. BioMetals 16:263–270

Bakker PAHM, Pieterse CMJ, van Loon LC (2007) Induced systemic resistance by fluorescent *Pseudomonas* spp. Phytopathol 97:239–243

Braun V (1997) Avoidance of iron toxicity through regulation of bacterial iron transport. Biol Chem 378:779–786

Briskot G, Taraz K, Budzikiewicz H (1989) Pyoverdine-type siderophores from *Pseudomonas aeruginosa*. Liebigs Ann Chem 1989:375–384

Brown SD, Utturkar SM, Klingeman DM, Johnson CM, Martin SL, Land ML, Lu T-YS, Schadt CW, Doktycz MJ, Pelletier DA (2012) Twenty-one genome sequences from *Pseudomonas* species and 19 genome sequences from diverse bacteria isolated from the rhizosphere and endosphere of *Populus deltoids*. J Bacteriol 194:5991–5993

Budzikiewicz H (1997) Siderophores of fluorescent pseudomonads. Z Naturforsch 52:713–720

Budzikiewicz H (2004) Siderophores of the Pseudomonadaceae *sensu stricto* (fluorescent and non-fluorescent *Pseudomonas* spp.). Prog Chem Org Nat Prod 87:81–237

Budzikiewicz H, Schröder H, Taraz K (1992) Zur Biogenese der *Pseudomonas*-siderophore: der Nachweis analoger Strukturen eines Pyoverdin-Desferribactin-Paares. Z Naturforsch C 47:26–32

Budzikiewicz H, Schäfer M, Fernández DU, Matthijs S, Cornelis P (2007) Characterization of the chromophore of pyoverdins and related siderophores by electrospray tandem mass spectrometry. Biometals 20:135–144

Cheng X, de Bruijn I, van der Voort M, Loper JE, Raaijmakers JM (2013) The Gac regulon of *Pseudomonas fluorescens* SBW25. Environ Microbiol Rep 5:608–619

Cornelis P, Bodilis J (2009) A survey of TonB-dependent receptors in fluorescent pseudomonads. Environ Microbiol Rep 1:256–262

Cornelis P, Matthijs S (2002) Diversity of siderophore-mediated iron uptake systems in fluorescent pseudomonads: not only pyoverdines. Environ Microbiol 4:787–798

Cox CD, Graham R (1979) Isolation of an iron-binding compound from *Pseudomonas aeruginosa*. J Bacteriol 137: 357–364

De Vleesschauwer D, Höfte M (2009) Rhizobacteria-induced systemic resistance. Plant Innate Immunity 51:223–281

Delorme S, Lemanceau P, Christen R, Corberand T, Meyer JM, Gardan L (2002) *Pseudomonas lini* sp. nov., a novel species from bulk and rhizospheric soils. Int J Syst Evol Microbiol 52:513–523

Dennis JJ, Zylstra GJ (1998) Plasposons: modular self-cloning minitransposon derivatives for rapid genetic analysis of gram-negative bacterial genomes. Appl Environ Microbiol 64:2710–2715

Duijff BJ, Recorbet G, Bakker PAHM, Loper JE, Lemanceau P (1999) Microbial antagonism at the root level is involved in the suppression of fusarium wilt by the combination of nonpathogenic *Fusarium oxysporum* Fo47 and *Pseudomonas putida* WCS358. Phytopathol 89:1073–1079

Edwards U, Rogall T, Blöcker H, Emde M, Böttger EC (1989) Isolation and direct complete nucleotide determination of entire genes, characterization of a gene coding for 16S ribosomal RNA. Nucl Acids Res 17:7843–7853

Fernández DU, Fuchs R, Taraz K, Budzikiewicz H, Munsch P, Meyer J-M (2001) Structure of a pyoverdine produced by a *Pseudomonas tolaasii*-like isolate. Biometals 14:81–84

Fuchs R, Budzikiewicz H (2001) Rearrangement reactions in the electrospray ionization mass spectra of pyoverdins. Int J Mass Spectrom 201(211):603–612

Galet J, Deveau A, Hôtel L, Frey-Klett P, Leblond P, Aigle B (2015) *Pseudomonas fluorescens* pirates both ferrioxamine and ferri-coelichelin siderophores from *Streptomyces ambofaciens*. Appl Environ Microbiol 81:3132–3141

Gasser I, Müller H, Berg G (2009) Ecology and characterization of polyhydroxyalkanoate-producing microorganisms on and in plants. FEMS Microbiol Ecol 70:142–150

Hartney SL, Mazurier S, Kidarsa TA, Quecine MC, Lemanceau P, Loper JE (2011) TonB-dependent outer-membrane proteins and siderophore utilization in *Pseudomonas fluorescens* Pf-5. Biometals 24:193–213

Höfte M, Seong KY, Jurkevitch E, Verstraete W (1991) Pyoverdine production by the plant growth beneficial *Pseudomonas* strain 7NSK2: ecological significance in soil. Plant Soil 130:249–257

Jurkevitch E, Hadar Y, Chen Y (1992) Differential siderophore utilization and iron uptake by soil and rhizosphere bacteria. Appl Environ Microbiol 58:119–124

Kloepper JW, Leong J, Teintze M, Schroth MN (1980) Enhanced plant growth by siderophores produced by plant growth-promoting rhizobacteria. Nature 286:885–886

Leeman M, den Ouden FM, van Pelt JA, Dirkx FPM, Steijl H, Bakker PAHM, Schippers B (1996) Iron availability affects induction of systemic resistance to *Fusarium* wilt of

radish *Pseudomonas fluorescens*. Phytopathology 85: 149–155

Lemanceau P, Expert D, Gaymard F, Bakker P, Briat JF (2009) Role of iron in plant-microbe interactions. Plant Innate Immunity 51:491–549

Long HH, Schmidt DD, Baldwin IT (2008) Native bacterial endophytes promote host growth in a species-specific manner; phytohormone manipulations do not results in common growth responses. PLoS One 3(7):e2702

Loper JE, Henkels MD (1997) Availability of iron to *Pseudomonas fluorescens* in rhizosphere and bulk soil evaluated with an ice nucleation reporter gene. Appl Environ Microbiol 63:99–105

Matthijs S, Baysse C, Koedam N, Abbaspour Tehrani K, Verheyden L, Budzikiewicz H, Schäfer M, Hoorelbeke B, Meyer J-M, De Greve H, Cornelis P (2004) The *Pseudomonas* siderophore quinolobactin is synthesized from xanthurenic acid, an intermediate of the kynurenine pathway. Mol Microbiol 52:371–384

Matthijs S, Abbaspour Tehrani K, Laus G, Jackson RW, Cooper RM, Cornelis P (2007) Thioquinolobactin, a *Pseudomonas* siderophore with antifungal and anti-*Pythium* activity. Environ Microbiol 9:425–434

Matthijs S, Budzikiewicz H, Schäfer M, Wathelet B, Cornelis P (2008) Ornicorrugatin, a new siderophore from *Pseudomonas fluorescens* AF76. Z Naturforsch C 63:8–12

Matthijs S, Laus G, Meyer JM, Abbaspour-Tehrani K, Schäfer M, Budzikiewicz H, Cornelis P (2009) Siderophore-mediated iron acquisition in the entomopathogenic bacterium *Pseudomonas entomophila*. Biometals 22:951–964

Matthijs S, Coorevits A, Gebrekidan TT, Tricot C, Vander Wauven C, Pirnay J-P, De Vos P, Cornelis P (2013) Evaluation of the *oprI* and *oprL* genes as molecular markers for the genus *Pseudomonas* and their use to study the biodiversity of a small Belgian River. Res Microbiol 164:254–261

Maurhofer M, Hase C, Meuwly P, Métraux JP, Défago G (1994) Induction of systemic resistance of tobacco to tobacco necrosis virus by the root-colonizing *Pseudomonas fluorescens* strain CHA0: influence of the *gacA* gene and of pyoverdine production. Phytopathol 84:39–146

Mercado-Blanco J, van der Drift KMGM, Olsson PE, Thomas-Oates JE, van Loon LC, Bakker PAHM (2001) Analysis of the *pmsCEAB* gene cluster involved in the biosynthesis of salicylic acid and the siderophore pseudomonine in the biocontrol strain *Pseudomonas fluorescens* WCS374. J Bacteriol 183:1909–1920

Meyer J-M, Abdallah MA (1978) The fluorescent pigment of *Pseudomonas fluorescens*: biosynthesis, purification and physicochemical properties. J Gen Microbiol 107:319–328

Meyer J-M, Geoffroy VA, Baida N, Gardan L, Izard D, Lemanceau P, Achouak W, Palleroni NJ (2002) Siderophore typing, a powerful tool for the identification of fluorescent and nonfluorescent pseudomonads. Appl Environ Microbiol 68:2745–2753

Meyer J-M, Gruffaz C, Raharinosy V, Bezverbnaya I, Schäfer M, Budzikiewicz H (2008) Siderotyping of fluorescent *Pseudomonas*: molecular mass determination *by mass* spectrometry as a powerful pyoverdine siderotyping method. Biometals 21:259–271

Moon CD, Zhang XX, Matthijs S, Schäfer M, Budzikiewicz H, Rainey PB (2008) Genomic, genetic and structural analysis of pyoverdine-mediated iron acquisition in the plant growth-promoting bacterium *Pseudomonas fluorescens* SBW25. BMC Microbiol 8:7

Mulet M, Bennasar A, Lalucat J, García-Valdés E (2009) An *rpoD*-based PCR procedure for the identification of *Pseudomonas* species and for their detection in environmental samples. Mol Cellul Prob 23:140–147

Mulet M, Lalucat J, García-Valdés E (2010) DNA sequence-based analysis of the *Pseudomonas* species. Environ Microbiol 12:1513–1530

Ongena M, Jacques P, Thonart P, Gwose I, Fernandez DU, Schäfer M, Budzikiewicz H (2001) The pyoverdin of *Pseudomonas fluorescens* BTP2, a novel structural type. Tetrahedron Lett 42:5849–5851

Poole K, Young L, Neshat S (1990) Enterobactin-mediated iron transport in *Pseudomonas aeruginosa*. J Bacteriol 172:6991–6996

Raaijmakers JM, Van Der Sluis I, Koster M, Bakker PAHM, Weisbeek PJ, Schippers B (1995) Utilization of heterologous siderophores and rhizosphere competence of fluorescent *Pseudomonas* spp. Can J Microbiol 41:126–135

Rausch C, Weber T, Kohlbacher O, Wohlleben W, Huson DH (2005) Specificity prediction of adenylation domains in nonribosomal peptide synthetases (NRPS) using transductive support vector machines (TSVM). Nucleic Acids Res 33:5799–5808

Risse D, Beiderbeck H, Taraz K, Budzikiewicz H, Gustine D (1998) Corrugatin, a lipopeptide from *Pseudomonas corrugata*. Z Naturforsch C 53:295–304

Schlegel K, Fuchs R, Schäfer M, Taraz K, Budzikiewicz H, Geoffroy V, Meyer JM (2001) The pyoverdins of *Pseudomonas* sp. 96-312 and 96-318. Z Naturforsch C 56:680–686

Schnider-Keel U, Seematter A, Maurhofer M, Blumer C, Duffy B, Gigot-Bonnefoy C, Reimmann C, Notz R, Défago G, Haas D, Keel C (2000) Autoinduction of 2,4-diacetylphloroglucinol biosynthesis in the biocontrol agent *Pseudomonas fluorescens* CHA0 and repression by the bacterial metabolites salicylate and pyoluteorin. J Bacteriol 182:1215–1225

Schwyn B, Neilands JB (1987) Universal chemical assay for the detection and determination of siderophores. Anal Biochem 160:47–56

Singh GM, Fortin PD, Koglin A, Walsh CT (2008) Beta-Hydroxylation of the aspartyl residue in the phytotoxin syringomycin E: characterization of two candidate hydroxylases AspH and SyrP in *Pseudomonas syringae*. Biochemistry 47:11310–11320

Stachelhaus T, Mootz HD, Marahiel MA (1999) The specificity-conferring code of adenylation domains in nonribosomal peptide synthetases. Chem Biol 6:493–505

Sultana R, Fuchs R, Schmickler H, Schlegel K, Budzikiewicz H, Siddiqui BS, Geoffroy V, Meyer JM (2000) A pyoverdine from *Pseudomonas* sp. CFML 95-275. Z Naturforsch C 55:857–865

Tamura K, Peterson D, Peterson N, Stecher G, Nei M, Kumar S (2011) MEGA5: molecular evolutionary genetics analysis using maximum like-lihood, evolutionary distance, and

maximum parsimony methods. Mol Biol Evol 28: 2731–2739

Tappe R, Taraz K, Budzikiewicz H, Meyer JM, Lefèvre JF (1993) Structure elucidation of a pyoverdin produced by *Pseudomonas aeruginosa* ATCC 27853. J Prakt Chem 335:83–87

Uría-Fernández D, Geoffroy V, Schäfer M, Meyer JM, Budzikiewicz H (2003) Structure revision of pyoverdines produced by plant-growth promoting and plant deleterious *Pseudomonas* species. Monatsh Chem 134:1421–1431

Van Der Voort M, Meijer HJ, Schmidt Y, Watrous J, Dekkers E, Mendes R, Dorrestein PC, Gross H, Raaijmakers JM (2015) Genome mining and metabolic profiling of the rhizosphere bacterium *Pseudomonas* sp SH-C52 for antimicrobial compounds. Front Microbiol 6:693

Vieira J, Messing J (1991) New pUC-derived cloning vectors with different selectable markers and DNA replication origins. Gene 100:189–194

Voisard C, Bull C, Keel C, Laville J, Maurhofer M, Schnider U, Défago G, Haas D (1994) Biocontrol of root diseases by *Pseudomonas fluorescens* CHA0: current concepts and experimental approaches. In: O'Gara F, Dowling D, Boesten B (eds) Molecular ecology of rhizosphere microorganisms. VCH, Weinheim, pp 67–89

Yamamoto S, Ksai H, Arnold DL, Jackson RW, Vivian A, Harayama S (2000) Phylogeny of the genus *Pseudomonas*: intrageneric structure reconstructed from the nucleotide sequences of *gyrB* and *rpoD* genes. Microbiology 146:2385–2394

Ye L, Ballet S, Hildebrand F, Laus G, Guillemyn K, Raes J, Matthijs S, Martins J, Cornelis P (2013) A combinatorial approach to the structure elucidation of a pyoverdine siderophore produced by a *Pseudomonas putida* isolate and the use of pyoverdine as a taxonomic marker for typing *P. putida* subspecies. Biometals 26:561–575

Ye L, Matthijs S, Bodilis J, Hildebrand H, Raes J, Cornelis P (2014a) Analysis of the draft genome of *Pseudomonas fluorescens* ATCC 17400 indicates a capacity to take up iron from a wide range of sources, including different exogenous pyoverdines. Biometals 27:633–644

Ye L, Hildebrand F, Dingemans J, Ballet S, Laus G, Matthijs S, Berendsen R, Cornelis P (2014b) Draft genome sequence analysis of a *Pseudomonas putida* W15Oct28 strain with antagonistic activity to Gram-positive and *Pseudomonas* sp. pathogens. PLoS One 9(11):e110038

Zerbino DR, Birney E (2008) Velvet: algorithms for *de novo* short read assembly using de Bruijn graphs. Genome Res 18:821–829